Inorg. Chem. **2002**, *41*, 5866–5873

Iron Complexes of 5,10,15,20-Tetraphenyl-21-oxaporphyrin

Miłosz Pawlicki and Lechosław Latos-Grażyński*

Department of Chemistry, University of Wrocław, 50 383 Wrocław, Poland

Received May 14, 2002

The iron complexes of 5,10,15,20-tetraphenyl-21-oxaporphyrin (OTPP)H have been investigated. Insertion of iron(II) followed by one-electron oxidation yielded a high-spin, six-coordinate $(OTPP)Fe^{III}Cl_2$ complex. The reduction of $(OTPP)Fe^{III}Cl_2$ has been accomplished by means of moderate reducing reagents producing high-spin five-coordinate $(OTPP)Fe^{II}Cl$. The molecular structure of $(OTPP)Fe^{III}Cl_2$ has been determined by X-ray diffraction. The iron(III) 21-oxaporphyrin skeleton is essentially planar. The furan ring coordinates in the η^1 fashion through the oxygen atom, which acquires trigonal geometry. The iron(III) apically coordinates two chloride ligands. Addition of potassium cyanide to a solution of $(OTPP)Fe^{III}Cl_2$ in methanol-d_4 results in its conversion to a six-coordinate, low-spin complex $[OTPP)Fe^{III}(CN)_2]$ which is spontaneously reduced to $[OTPP)Fe^{II}(CN)_2]^-$ by excess cyanide. The spectroscopic features of $[OTPP)Fe^{III}(CN)_2]$ correspond to the common low-spin iron(III) porphyrin $(d_{xy})^2(d_{xz}d_{yz})^3$ electronic configuration. Titration of $(OTPP)Fe^{III}Cl_2$ or $(OTPP)Fe^{II}Cl$ with *n*-BuLi (toluene-d_8, 205 K) resulted in the formation of $(OTPP)Fe^{II}(CH_2CH_2CH_2CH_3)$. $(OTPP)Fe^{II}$(*n*-Bu) decomposes via homolytic cleavage of the iron–carbon bond to produce $(OTPP)Fe^{I}$. The EPR spectrum (toluene-d_8, 77 K) is consistent with a $(d_{xy})^2(d_{xz})^2(d_{yz})^2(d_{z^2})^1(d_{x^2-y^2})^0$ ground electronic state of iron(I) oxaporphyrin ($g_1 = 2.234$, $g_2 = 2.032$, $g_3 = 1.990$). The ^{1}H NMR spectra of $(OTPP)Fe^{III}Cl_2$, $(OTPP)Fe^{III}(CN)_2$, $\{[(OTPP)Fe^{III})]_2O\}^{2+}$, and $(OTPP)Fe^{II}Cl$ have been analyzed. There are considerable similarities in ^{1}H NMR properties within each iron(*n*) oxaporphyrin–iron(*n*) regular porphyrin or *N*-methylporphyrin pair ($n = 2$, 3). Contrary to this observation, the pattern of downfield positions of pyrrole resonances at 156.2, 126.5, 76.3 ppm and furan resonance at 161.4 ppm (273 K) detected for the two-electron reduction product of $(OTPP)Fe^{III}Cl_2$ is unprecedented in the group of iron(I) porphyrins.

Introduction

Core-modified porphyrins are formally related to regular porphyrins by a replacement of a NH fragment by a heteroatom typically from group 16 of the periodic table.[1−4] In the macrocyclic environment, a heteroatom can function as a donor toward a variety of metal ions, offering an insight into coordination properties of furan, thiophene, or selenophene, respectively.[2] The presence of the heavier heteroatoms shrinks the coordination core of heteroporphyrin in comparison to regular porphyrins. Matching the cavity size of a macrocycle to the ionic radius of a metal is of prime importance when considering complex formation between a metal and the complexing porphyrin or heteroporphyrin.[1,2] Only in 21-oxaporphyrin, 21,23-dioxaporphyrin, and 21-oxacorrole is the size of the coordinating center comparable with that of regular porphyrins, because the atomic radii of nitrogen and oxygen are similar.[5−7] In these terms, the situation is radically different for 21-thiaporphyrin or 21-selenaporphyrin as reflected by remarkable differences in the observed 21-oxaporphyrin and 21-thiaporphyrin or 21-selenaporphyrin coordination modes.[2,6,8,9]

The coordination chemistry of heteroporphyrins has been explored for a number of metal ions: for 21-oxaporphyrin, Ni(II),[6] Ni(I),[6] Zn(II),[10] Co(II),[10] Mn(II),[10] Cu(II);[11] for 21-

* To whom correspondence should be addressed. E-mail: LLG@wchuwr.chem.uni.wroc.pl.

(1) Latos-Grażyński, L.; Chmielewski, P. J. *New J. Chem.* **1997**, *21*, 691.
(2) Latos-Grażyński, L. Core Modified Heteroanalogues of Porphyrins and Metalloporphyrins. In *The Porphyrin Handbook;* Kadish, K. M., Smith, K. M., Guilard, R., Eds.; Academic Press: New York, 2000; Vol. 2, p 361.
(3) Vogel, E. *Pure Appl. Chem.* **1993**, *66*, 143.
(4) Vogel, E. *J. Heterocycl. Chem.* **1996**, 33, 1461.
(5) Latos-Grażyński, L.; Pacholska, E.; Chmielewski, P.; Olmstead, M. M.; Balch, A. L. *Angew. Chem., Int. Ed. Engl.* **1995**, *34*, 2252.
(6) Chmielewski, P. J.; Latos-Grażyński, L.; Olmstead, M. M.; Balch, A. L. *Chem. Eur. J.* **1997**, *3*, 268.
(7) Sridevi, B.; Narayanan S. J.; Chandrashekar, T. K. *Chem. Eur. J.* **2000**, *6*, 2554.
(8) Latos-Grażyński; L.; Lisowski, J.; Olmstead, M. M.; Balch, A. L. *Inorg. Chem.* **1989**, *28*, 1183.
(9) Latos-Grażyński, L.; Pacholska, E.; Chmielewski, P. J.; Olmstead, M. M.; Balch, A. L. *Inorg. Chem.* **1996**, *35*, 566.

10.1021/ic025718p CCC: $22.00
Published on Web 10/02/2002

thiaporphyrin, Li(I),[12] Cu(II),[13,14] Ni(II),[8] Ni(I),[15] Fe(II),[8] Pd-(II),[16] Rh(III);[17] for 21-selenaporphyrin, Ni(II);[9] for 21,23-dioxaporphyrin, Ni(II);[6,18] for 21-oxa-23-thiaporphyrin, Cu(II);[11] and for 21,23-dithiaporphyrin, Ru(II).[19] This laboratory has systematically examined the coordination chemistry of nickel heteroporphyrins.[1,2,6,8,15,17] It was determined that heteroporphyrins stabilize the uncommon nickel(I).[6,15] Once the nickel-(II) ion was located in the heteroporphyrin macrocycle, the extremely rare high-spin organonickel(II) complexes could be trapped and identified.[20−22] Organometallic chemistry of nickel(II) and stabilization of nickel(I) attracted much attention in light of their biochemical implications. Suggested participation of analogous species in the mechanisms of reactions of methyl-S-coenzyme-M reductase provided some motivation for the effort in this direction.[23,24]

There has been relative little attention given to iron heteroporphyrins despite the extensive search for suitable porphyrins and metalloporphyrins to act as biomimetic models of the multiple fundamental biochemical roles played by iron protoporphyrin IX.[25] In the single case studied, it was found that high-spin iron(II) 21-thiaporphyrin is a five-coordinate complex where the thiophene ring coordinates in the side-on fashion.[8]

Because of the size of the coordinating core and the feasible in-plane coordination of the furan ring, the 21-oxaporphyrin provides the most suitable environment to explore iron chemistry. In comparison to regular iron porphyrins, the properties of iron 21-oxaporphyrin are expected to reflect the influence of the decreased anionic charge and the replacement of the nitrogen by the oxygen atom. Actually, the charge of the ligand and the size of the coordination resemble those of *N*-alkylporphyrins.[26] Thus, particularly in light of the rich and interesting chemistry of iron *N*-alkyl porphyrins,[27−32] here we report on the structure and spectroscopic properties of iron(*n*) 21-oxaporphyrins.

Chart 1

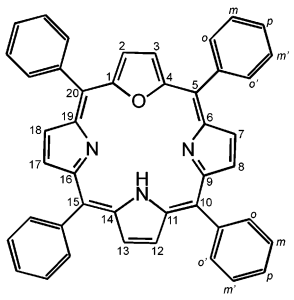

^{1}H NMR spectroscopy was shown to be a definitive method for detecting and characterizing iron porphyrins[33] and iron(*n*) N-substituted porphyrins[26−29,31−33] at different coordination/oxidation states. Consequently, we have explored the relation between the coordination geometry and isotropic shifts in a series of iron(*n*) 21-oxaporphyrins.

Results and Discussion

Formation and Characterization of Iron(III) Complexes. Insertion of iron into 5,10,15,20-tetraphenyl-21-oxaporphyrin (OTPP)H (Chart 1) has been readily achieved by addition of a methanol solution of iron(II) chloride hydrate to a chloroform solution of the ligand. The presence of methanol is essential for metalation and facilitates the reaction by producing soluble forms of iron(II). The reaction results in the formation of a six-coordinate (OTPP)$Fe^{III}Cl_2$ complex. Presumably, the originally formed (OTPP)$Fe^{II}Cl$ is oxidized in the presence of dioxygen after the insertion step has occurred. (OTPP)$Fe^{III}Cl_2$ is stable as a solid and in solution. It has good solubility in chloroform, methylene chloride, and toluene.

Moderate reducing reagents are sufficient to carry out one-electron reduction of (OTPP)$Fe^{III}Cl_2$. Reduction in chloroform by aqueous sodium dithionite or zinc amalgam produces iron(II) derivatives. To avoid any complication with axial ligation, zinc amalgam has been used for the preparative reduction according to the reaction:

$$(\mathrm{OTPP})\mathrm{Fe^{III}Cl_2} + \mathrm{e^-} \rightarrow (\mathrm{OTPP})\mathrm{Fe^{II}Cl} + \mathrm{Cl^-} \qquad (1)$$

The chemical reduction is reversible. Addition of oxidizing reagents (Br_2, I_2) regenerates the iron(III) complexes. The progress of the reaction was conveniently followed by

(10) Broadhurst, M. J.; Grigg, R.; Johnson, A. W. *J. Chem. Soc. C* **1971**, 3681.
(11) Sridevi, B.; Narayanan, S. J.; Srinivasan, A.; Chandrashekar, T. K.; Subramanian, J. *J. Chem. Soc., Dalton Trans.* **1998**, 1979.
(12) Gebauer, A.; Schmidt, J. A. R.; Arnold, J. *Inorg. Chem.* **2000**, *39* 3424.
(13) Latos-Grażyński, L.; Lisowski, J.; Olmstead, M. M.; Balch, A. L. *J. Am. Chem. Soc.* **1987**, *109*, 4428.
(14) Lisowski, J.; Grzeszczuk, M.; Latos-Grażyński, L. *Inorg. Chim. Acta* **1989**, *161*, 153.
(15) Chmielewski, P. J.; Grzeszczuk, M.; Latos-Grażyński, L.; Lisowski, J. *Inorg. Chem.* **1989**, *28*, 3546.
(16) Latos-Grażyński, L.; Lisowski, J.; Chmielewski, P. J.; Grzeszczuk, M.; Olmstead, M. M.; Balch, A. L. *Inorg. Chem.* **1994**, *33*, 192.
(17) Latos-Grażyński, L.; Lisowski, J.; Olmstead, M. M.; Balch, A. L. *Inorg. Chem.* **1989**, *28*, 3328.
(18) Gross, Z.; Saltsman, I.; Pandian, R. P.; Barzilay, C. *Tetrahedron Lett* **1997**, *38*, 2383.
(19) Hung, C.-H.; Ou, C.-K.; Lee, G.-H.; Peng, S.-M. *Inorg. Chem.* **2001**, *40*, 6854.
(20) Chmielewski, P. J.; Latos-Grażyński, L. *Inorg. Chem.* **1992**, *31*, 5231.
(21) Pacholska, E.; Chmielewski, J. P.; Latos-Grażyński, L. *Inorg. Chim. Acta* **1998**, *273*, 184.
(22) Chmielewski, P. J.; Latos-Grażyński, L. *Inorg. Chem.* **1998**, *37*, 4179.
(23) Jaun, B. In *Metal Ions in Biological Systems*; Sigel, H., Sigel, A., Eds.; Marcel Dekker: New York, 1993; Vol. 29, p 287.
(24) Ermler, U.; Grabarse, W.; Shima, S.; Goubeaud, M.; Thauer, R. K. *Science* **1997**, *278*, 1457.
(25) Biochemistry and Binding. In *The Porphyrin Handbook*; Kadish, K. M., Smith, K. M., Guilard, R., Eds.; Academic Press: New York, 2000; Vol. 4.
(26) Lavallee, D. K. *The Chemistry and Biochemistry of N-substituted Porphyrins*; VCH: New York, 1987.
(27) Balch; A. L.; Chang; Y.-W.; La Mar; G. N.; Latos-Grażyński, L.; Renner, M. W. *Inorg. Chem.* **1985**, *24*, 1437.
(28) Balch; A. L.; La Mar; G. N.; Latos-Grażyński, L.; Renner, M. W. *Inorg. Chem.* **1985**, *24*, 2432.
(29) Wysłouch, A.; Latos-Grażyński, L.; Grzeszczuk, M.; Drabent, K.; Bartczak, T. *Chem. Commun.* **1988**, 1377.
(30) Bartczak, T.; Latos-Grażyński, L.; Wysłouch A. *Inorg. Chim. Acta* **1990**, *171*, 205.
(31) Balch, A. L. Cornman, C. R.; Latos-Grażyński, L.; Olmstead, M. M. *J. Am. Chem. Soc.* **1990**, *112*, 7552.
(32) Balch, A. L.; Cornman, C. R.; Latos-Grażyński, L.; Renner, M. W. *J. Am. Chem. Soc* **1992**, *114*, 2230.
(33) Walker, F. A. Proton NMR Spectroscopy of Paramagnetic Metalloporphyrins. In *The Porphyrin Handbook*; Kadish, K. M., Smith, K. M., Guilard, R., Eds.; Academic Press: New York, 2000; Vol. 5, p 81.

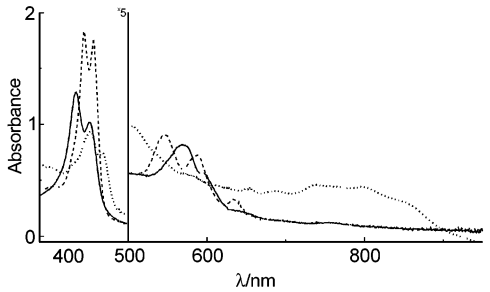

Figure 1. UV−vis spectra of iron(*n*) 21-oxaporphyrin complexes in dichloromethane: (OTPP)$Fe^{III}Cl_2$ (—), (OTPP)$Fe^{II}Cl$ (---), and (OTPP)-Fe^{I}(toluene) (···).

electronic spectroscopy. The electronic absorption spectra of (OTPP)$Fe^{III}Cl_2$ and (OTPP)$Fe^{II}Cl$ are shown in Figure 1. Metalloporphyrin-like spectra are clearly present for both complexes with a split Soret band and two (iron(III)) or three (iron(II)) broad Q-bands, respectively.

The cyclic voltammetry experiment has been carried out. The half-wave potentials for the two one-electron reductions of (OTPP)$Fe^{III}Cl_2$ equal (1) 0.595 and (2) −0.895 (in V vs Ag/AgCl, CH_2Cl_2 solution, TBAP). Consequently, the first reductions can be assigned to the Fe^{III}/Fe^{II} metal-centered processes. Cyclic voltammetry revealed that there is significant stabilization of the divalent oxidation state in the iron 21-oxaporphyrin complex in comparison to regular iron porphyrins. For instance, for (TPP)$Fe^{III}Cl$, the reduction potential for Fe(III) to Fe(II) equals −0.121 V (DMF vs Ag/AgCl).[34] Interestingly, the analogous reduction potential for $(NCH_3TPP)Fe^{III}Cl^+$ equals 0.51 V (vs Ag/AgCl).[35] The second half-wave potential may be accounted for the (OTPP)-Fe^{II}/(OTPP)Fe^{I} couple or, alternatively, for $(OTPP^{\bullet-})Fe^{II}$/(OTPP)Fe^{II}.

Crystal Structure of (OTPP)$Fe^{III}Cl_2$. The structure has been studied by X-ray diffraction. The perspective views of the complex are shown in Figure 2.

The structure of (OTPP)$Fe^{III}Cl_2$ displays disorder in the location of furan oxygen and pyrrolic nitrogens. The structure has been refined to give 25% occupancy with oxygen and 75% occupancy with nitrogen at each five-membered ring. The iron(III) 21-oxaporphyrin skeleton is essentially planar. Thus, the iron(III) is coplanar with the furan ring. It implies that the furan ring is planar and coordinates in the η^1 fashion through the oxygen atom which acquires trigonal geometry. The Fe^{III}−Cl(1) (2.302(1) Å) and Fe^{III}−Cl(2) (2.302(1) Å) distances are among the longest found for high-spin iron(III) porphyrins (e.g., in (TPP)$Fe^{III}Cl$, Fe^{III}−Cl 2.218(6) Å).[36] This is a considerable lengthening of the Fe^{III}−Cl bonds which can readily be ascribed to the mutual *trans* interaction of axial chloride ligands. A similar phenomenon was previously observed in the (β-PPh_3-TPP)$Fe^{III}Cl_2$ structure (Fe^{III}−Cl, 2.429(3) and 2.348(3) Å).[37]

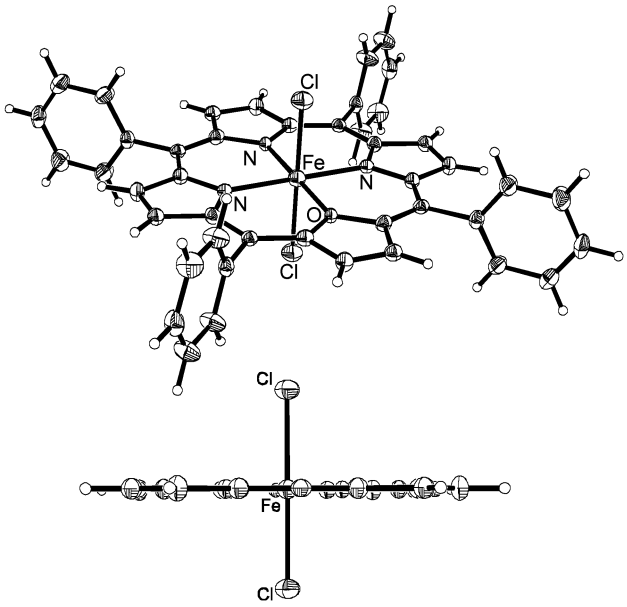

Figure 2. Perspective drawing (with 50% probability ellipsoids) of (OTPP)$Fe^{III}Cl_2$ showing one of the molecular orientations. The lower view in which aryl groups are omitted emphasizes the planarity of the macrocycle.

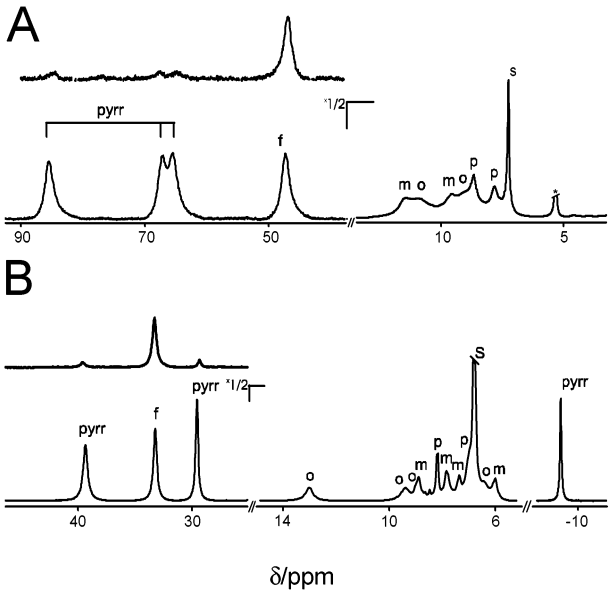

Figure 3. ^{1}H NMR spectra (298 K, $CDCl_3$) of (A) (OTPP)$Fe^{III}Cl_2$ and (B) (OTPP)$Fe^{II}Cl$. Insets show spectra for (OTPP-d_6)$Fe^{III}Cl_2$ and (OTPP-d_6)$Fe^{II}Cl$, respectively. The pyrrole, furan, and *ortho*, *meta*, and *para* resonances are labeled pyrr, f, o, m, p, respectively.

^{1}H NMR Studies of High-Spin Iron(II) and Iron(III) 21-Oxaporphyrins. The ^{1}H NMR spectra of the paramagnetic (OTPP)$Fe^{III}Cl_2$ and (OTPP)$Fe^{II}Cl$ are shown at Figure 3. The spectral parameters for these and other relevant compounds are gathered in Table 1.

The spectroscopic data for iron 21-oxaporphyrins have been analyzed through the consideration of their effective symmetry in solution. (OTPP)$Fe^{III}Cl_2$ appears to have the effective C_{2v} geometry with one of the mirror planes passing through the iron, chloride, and the furan oxygen. In this case, there are three distinct pyrrole protons and one furan proton. Their *ortho* and *meta* positions are pairwise equivalent because of the mirror symmetry with respect to the porphyrin

(34) Donohoe, R. J.; Atamian, M.; Bocian, D. F. *J. Am. Chem. Soc*. **1987**, *109*, 5593.
(35) Anderson, O. P.; Kopelove, A. B.; Lavallee, D. *Inorg. Chem.* **1980**, *19*, 2101
(36) Hoard, J. L.; Cohen, G. H.; Glick, M. D. *J. Am. Chem. Soc*. **1967**, *89*, 1992
(37) Małek, A.; Latos-Grażyński, L.; Bartczak, T.; Ząd̷ło, A. *Inorg. Chem.* **1991**, *30*, 3222.

Table 1. Chemical Shifts of Iron(*n*) Oxaporphyrins[a]

	furan	pyrrole			*meso*-phenyl
$[(OTPP)Fe^{III}Cl_2]$[b]	47.7	66.3	67.9	86.2	10.9(*o*), 11.5(*m*), 9.1(*o*), 9.6(*m*), 8.7(*p*), 7.8(*p*)
$[(OTPP)Fe^{II}Cl]$[b]	33.2	39.3	29.5	−6.4	13.1(*o*), 9.7(*o*), 9.3(*o*), 9.2(*m*), 8.6(*p*), 8.2(*m*), 7.8(*m*), 7.4(*p*), 6.9(*o*), 6.5(*m*),
$[(OTPP)Fe^{III}(CN)_2]$[b]	−5.4	−16.2	−24.6	−40.5	6.8(*p*), 6.5(*m*), 6.2(*p*), 6.1(*m*), 5.9(*o*), 4.6(*o*),
$[(ODPDTP)Fe^{II}(CN)_2]^{-}$ [b]	8.56(*s*)	8.40(*d*)	8.35(*d*)	8.06(*s*)	7.99(*o*), 7.93(*o*), 7.66(*m*,*p*), 7.55(*m*), 2.64(pCH_3)
$[(OTPP)Fe^{II}$*n*-Bu][c,e]	7.75(*s*)	7.65(*d*)	7.58(*d*)	7.04(*s*)	8.04(2^x*o*), 7.78(*o*), 7.5(*o*),7.41(*m*), 7.31 (2^x*p*,*m*)7.21(*m*),
[(OTPP)Fe][d,e]	161.4	156.2	129.5	76.3	22(*o* or *m*),21.3(*o* or *m*), 12.6(*p*), 12.4(*p*)

[a] Unless otherwise indicated, all compounds measured in chloroform-*d*. [b] 295 K. [c] 215 K (α-CH_2, −5.96 ppm; β-CH_2, −1.64 ppm; γ-CH_2, −0.36 ppm; δ-CH_3, 0.12 ppm). [d] −273 K. [e] Measured in toluene-d_8.

plane. However, for $(OTPP)Fe^{II}Cl$, the symmetry lowers to C_s, and two *ortho* and two *meta* positions on each phenyl ring will be distinguishable by ^{1}H NMR unless the rotation around the $C_{meso}-C_\alpha$ bond is sufficiently fast.[33]

Apart from these geometrical considerations, the resonance assignments, which are given above each peak in Figure 3, have been made on the basis of relative intensities, line widths, and site specific deuteration. To distinguish the pyrrole and furan resonances, the ^{1}H NMR spectra of pyrrole-deuterated $(OTPP\text{-}d_6)Fe^{III}Cl_2$ and $(OTPP\text{-}d_6)Fe^{II}Cl$ have been obtained and are shown in insets of Figure 3, respectively. The three pyrrole resonances of $(OTPP)Fe^{III}Cl_2$ are in the 90−60 ppm region (298 K) which is typical for high-spin iron(III) tetraarylporphyrins[33,38] and *N*-methylporphyrins.[28,31] The furan resonance is located at 47.7 ppm.

Curie plots for pyrrole and furan resonances of $(OTPP)Fe^{III}Cl_2$ and $(OTPP)Fe^{II}Cl$ (See Supporting Information) show linear behaviors, but the extrapolated intercepts are fairly far from the diamagnetic positions of $[(OTPP)Fe^{II}(CN)_2]^-$ (Table 1). Significantly, the deviations from the Curie law differ for each pyrrolic position.

One-electron reduction of $(OTPP)Fe^{III}Cl_2$ to $(OTPP)Fe^{II}Cl$ resulted in characteristic spectroscopic changes. In this case, the furan resonance has been unambiguously identified at 33.2 ppm because it is present in the ^{1}H NMR spectrum of $(OTPP\text{-}d_6)Fe^{II}Cl$ where the ligand is deuterated in all β-pyrrole positions. (Figure 3, trace B; Table 1). Two pyrrole resonances are shifted downfield, and one is shifted upfield. The upfield position of the regular pyrrole resonance was previously found for iron(II) *N*-methylporphyrin ($N\text{-}CH_3$-TPP)$Fe^{II}Cl$ and iron(II) 21-thiaporphyrin (STPP)$Fe^{II}Cl$.[8,27]

The paramagnetic shifts of the high-spin iron(III) and iron(II) 21-oxaporphyrins can be explained in terms typically applied to regular iron porphyrins and iron N-substituted porphyrins. In the case of a high-spin iron(III) center, $(d_{xy})^1(d_{xz}d_{yz})^2(d_{z^2})^1(d_{x^2-y^2})^1$, both σ and π delocalization routes of spin density can operate. The domination of the σ route results in the downfield shifts of pyrrole resonances as seen for $(OTPP)Fe^{III}Cl_2$.[31,33,38,39]

The observed pyrrole and furan hyperfine shifts of $(OTPP)Fe^{II}Cl$ are consistent with the high-spin iron(II) $(d_{xy})^2(d_{xz})^1(d_{yz})^1(d_{z^2})^1(d_{x^2-y^2})^1$ ground electronic state. The pattern for the contact shift arises from the cancellation of effects of unpaired spin density resulting from spin delocalization in σ as well as both filled and vacant π molecular orbitals corresponding to 3π and 4π* orbitals of the regular porphyrin.[27,39,40]

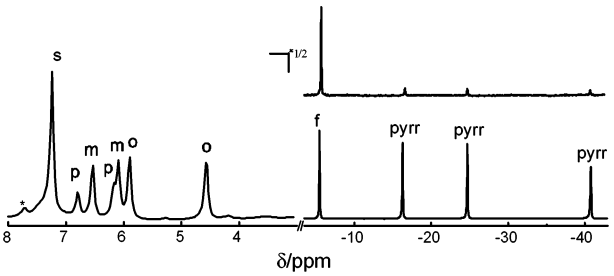

Figure 4. ^{1}H NMR spectrum of $(OTPP)Fe^{III}(CN)_2$ (298 K, $CDCl_3$). Labeling follows that in Figure 3. Inset shows spectrum for $(OTPP\text{-}d_6)$-$Fe^{III}(CN)_2$.

^{1}H NMR Characterization of Low-Spin Iron(III) Porphyrins. Addition of potassium cyanide in excess to a solution of $(OTPP)Fe^{III}Cl_2$ in methanol-d_4 results in its conversion to six-coordinate low-spin complex $[(OTPP)Fe^{III}$-$(CN)_2]$. The representative ^{1}H NMR spectrum for $[(OTPP)$-$Fe^{III}(CN)_2]$ is shown in Figure 4.

The characteristic set of three upfield shifted pyrrole and one furan resonance of $[(OTPP)Fe^{III}(CN)_2]$ has been detected. These resonances are accompanied by a group of upfield shifted *ortho*, *meta*, and *para meso*-phenyl proton resonances. As usual for low-spin iron(III) porphyrins, formed by coordination of two cyanide ligands, this compound demonstrates very narrow paramagnetically shifted resonances due to the optimal relaxation properties.[33] The primary assignment could be made on the basis of the position of resonances, their intensities, deuteration, and the COSY map. The paramagnetic shifts of $[(OTPP)Fe^{III}(CN)_2]$ vary linearly with T^{-1} (see Supporting Information), but the extrapolated lines do not pass through the positions expected for the diamagnetic references.[33,37]

Under anaerobic conditions, the cyanide anion acts as a one-electron reducing reagent to produce the diamagnetic $[(OTPP)Fe^{II}(CN)_2]^-$ identified here by means of ^{1}H NMR (Table 1). Addition of dioxygen to the sample results in a slow formation of the μ-oxo diiron(III) derivative $\{[(OTPP)$-$Fe^{III}]_2O\}^{2+}$. Its identity is confirmed by a set of four new resonances arising at 16−12 ppm, that is, in the region typical for strongly antiferromagnetically coupled μ-oxo di-iron

(38) Wojaczyński, J.; Latos-Grażyński, L.; Hrycyk, H.; Pacholska, E.; Rachlewicz, K.; Szterenberg, L. *Inorg. Chem.* **1996**, *35*, 6861.

(39) La Mar, G.; Walker, F. A. In *The Porphyrins*; Dolphin, E. Ed.; Academic Press: New York, 1979; Vol. IVB, p 57.

(40) Lisowski, J.; Latos-Grażyński, L.; Szterenberg, L. *Inorg. Chem.* **1992**, *31*, 1933.

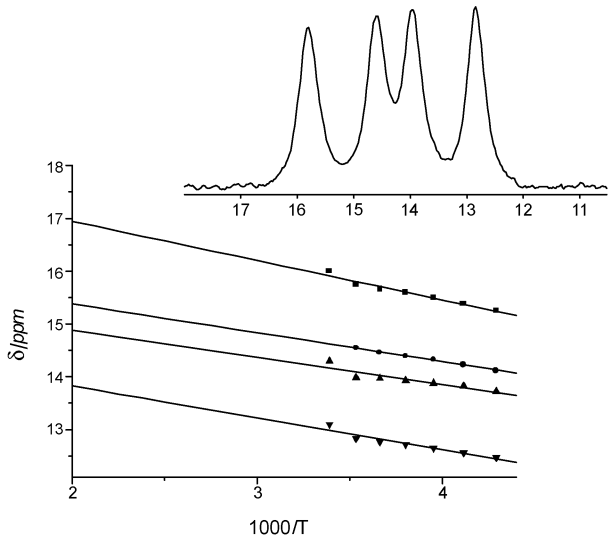

Figure 5. Plot of the chemical shift versus $1/T$ for $\{[(OTPP)Fe^{III}]_2O\}^{2+}$. Inset presents the pyrrolic fragment of the ^1H NMR spectrum (298 K, $CDCl_3$). The solid lines are for illustrative purpose only.

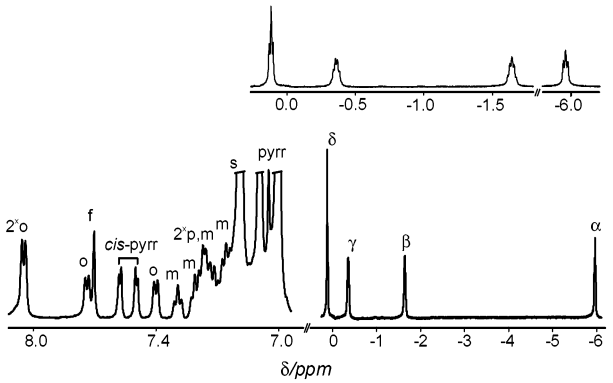

Figure 6. ^1H NMR spectrum of (OTPP)Fe^{II}(*n*-butyl) (215 K, toluene-d_8). Labeling follows that in Figure 3. The alkyl ligand resonances are labeled α, *β*, *δ*, *γ*. Inset shows the spin−spin splitting of the *n*-butyl chain.

porphyrin complexes.[29,33,39] An increase of the pyrrole and furan resonance shifts on warming reflects the anti-Curie behavior expected for such an electronic structure (Figure 5).[41] The reduction of (OTPP)$Fe^{III}(CN)_2$ by cyanide has the precedence in the reactivity of regular iron(III) porphyrins.[42]

Reaction with Carbanions. Treatment of (OTPP)Fe^{III}-Cl_2 in toluene-d_8 solution with *n*-butyllithium in hexane solution at 205 K results in the conversion to (OTPP)-$Fe^{II}(CH_2CH_2CH_2CH_3)$ (Figure 6).

The four resonances expected for a coordinated *n*-butyl group are present with the upfield ring current shifts which are similar to those of diamagnetic metalloporphyrin bearing axial alkyl ligands (α-CH_2, −5.96; *β*-CH_2, −1.64; *γ*-CH_2, −0.35; *δ*-CH_3, 0.12 ppm). It should be noticed that the spin−spin splittings expected for such a *n*-butyl ligand are clearly resolved and the scalar connectivity scheme was confirmed by the COSY experiment. The pyrrole and furan resonances are located at 7.75 (H2,3); 7.65, 7.58 (H7,H8), 7.04 (H12,-13) ppm, respectively.

Integration of the *β*-H and the axial ligand resonances indicates that one axial ligand is present in the iron(II) complexes. These spectral characteristics confirm that the iron(II) 21-oxaporphyrin alkyl complex is similar to known (TPP)Fe^{II}(*n*-propyl), (TPP)Fe^{II}(ethyl), and (Pc)Fe^{II}(alkyl) complexes.[43,44] Some upfield relocation of the pyrrole and furan resonances with respect to diamagnetic $[(OTPP)Fe^{II}(CN)_2]^-$ results presumably from a rapid electron exchange with a residual low-spin $[(OTPP)Fe^{III}(n\text{-Bu})]^-$. Alternatively, some admixture of the paramagnetic configuration to the ground electronic state of (OTPP)Fe^{II}(*n*-Bu) can be considered.

The formation of (OTPP)Fe^{II}(*n*-Bu) has been accounted for by a two-step process according to the following equations:

$$(OTPP)Fe^{III}Cl_2 + n\text{-BuLi} \rightarrow \{(OTPP)Fe^{III}Cl(n\text{-Bu})\} + LiCl \quad (2)$$

$$\{(OTPP)Fe^{III}Cl(n\text{-Bu})\} \rightarrow (OTPP)Fe^{II}Cl + Bu^{\bullet} \quad (3)$$

$$(OTPP)Fe^{II}Cl + n\text{-BuLi} \rightarrow (OTPP)Fe^{II}(n\text{-Bu}) + LiCl \quad (4)$$

Alkyllithium, aryllithium, or Grignard reagents are known to act as one-electron reducing reagents.[45−49] The reduction has been also demonstrated in several attempts to generate metalloporphyrins with metal−carbon bonds.[48,49] To clarify the point that the formation of (OTPP)Fe^{II}(*n*-Bu) from (OTPP)$Fe^{III}Cl_2$ has been preceded by one-electron reduction step, we have demonstrated that this species can be obtained by an independent route. Thus, the sample of (OTPP)Fe^{II}-Cl, obtained by reduction of (OTPP)$Fe^{III}Cl_2$ with zinc amalgam, was dissolved in toluene-d_8 and titrated with *n*-BuLi (205 K) to yield (OTPP)Fe^{II}(*n*-Bu). The observation of the solution behavior of (OTPP)Fe^{II}(*n*-Bu) revealed that this complex is thermally stable at 205 K. Warming of (OTPP)Fe^{II}(*n*-Bu) in toluene-d_8 resulted in its complete decomposition at 250 K after 45 min. The process yielded a new compound detected by ^1H NMR spectroscopy (Figure 7).

The formation of the new species can be accounted for by a homolytic cleavage of the iron−carbon bond according to the following reaction:

$$(OTPP)Fe^{II}(n\text{-Bu}) \rightarrow (OTPP)Fe^{I} + Bu^{\bullet} \quad (5)$$

Notably, (OTPP)Fe^{I} has been generated using the independent routes. Thus, the reduction of (OTPP)Fe^{II}Cl in toluene-d_8 with $NaBH_4$ in THF gives (OTPP)Fe^{I}. Treatment

(41) Boersma, A. D.; Goff, H. M. *Inorg. Chem.* **1984**, *23*, 1617.
(42) La Mar, G. N.; Del Gaudio, J. *Adv. Chem. Ser.* **1977**, *162*, 207.
(43) Balch, A. L.; Cornman, C. R.; Safari, N.; Latos-Grażyński, L. *Organometallics* **1990**, *9*, 2420.
(44) Tahiri, M.; Doppelt, P.; Fischer, J. Weiss, R. *Inorg. Chem.* **1988**, *27*, 2897.
(45) Cloutour, C.; Debaig-Valade, C.; Gacherieu, C.; Pommier, J.-C. *J. Organomet. Chem.* **1984**, *269*, 239.
(46) Staško, A.; Tkáč, A.; Malík, L.; Adamčík, V. *J. Organomet. Chem.* **1975**, *92*, 261.
(47) Kane, K. M.; Lemke, F. R.; Petersen, J. L. *Inorg. Chem.* **1997**, *36*, 1354.
(48) Chmielewski, P. J.; Latos-Grażyński, L. *Inorg. Chem.* **2000**, *39*, 5639.
(49) Balch, A. L.; Hart, R. H.; Latos-Grażyński, L.; Traylor, T. G. *J. Am. Chem. Soc.* **1990**, *112*, 7382.

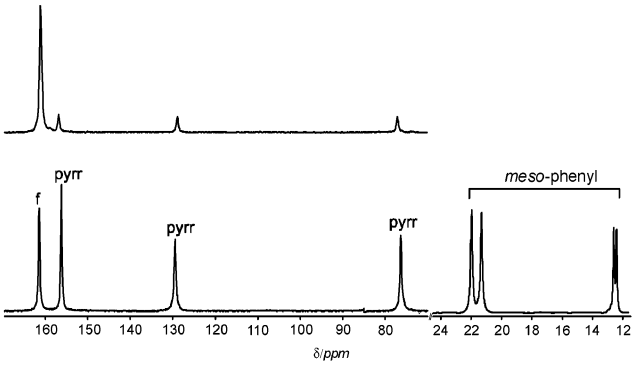

Figure 7. ^{1}H NMR spectrum of (OTPP)Fe^{I} (273 K, toluene-d_8). Labeling follows that in Figure 3. Inset shows spectrum for (OTPP-d_6)Fe^{I}.

of (OTPP)Fe^{III}Cl$_2$ with 2 equiv of PhMgBr yields (OTPP)-Fe^{I} directly and cleanly at 205 K. Generally, reactions of (OTPP)Fe^{III}Cl$_2$ with carbanions (toluene-d_8, 205 K) result in a significantly different ^{1}H NMR picture than that determined for the analogous experiment with the use of (TPP)Fe^{III}Cl and alkyl Grignard reagent or alkylithium reagents where low-spin (TPP)Fe^{III}(alkyl) or (TTP)Fe^{III}(aryl) or intermediate-spin (TPP)Fe^{II} was detected.[33,49,50] Typically, the reduction process of regular iron(III) porphyrins with alkyl reagents stops at the iron(II) oxidation level.

As the identical product can be generated using different reducing reagents, one unambiguously concludes that the reaction product does not contain any apically bound aryl or alkyl ligand. (OTPP)Fe^{I} is thermally stable in the 193−272 K temperature range. Addition of dioxygen results in the formation of (OTPP)Fe^{II}Cl or (OTPP)Fe^{II}Br as both anions are present in the reaction mixture, allowing us to conclude that the 21-oxaporphyrin ring remained intact in the reaction. Despite the apparent differences in oxidation states, the ^{1}H NMR spectrum of (OTPP)Fe^{I} bears some features of high-spin (OTPP)Fe^{III}Cl$_2$. Namely, the pyrrole and furan resonances are shifted strongly downfield. Actually, the shift values found for (OTPP)Fe^{I} are significantly higher than those determined for (OTPP)Fe^{III}Cl$_2$ at the same temperature. Noticeably, the furan resonance, which demonstrated the smallest shift for high-spin iron(III) species, presents the largest one in the case of (OTPP)Fe^{I}. Two sides of the 21-oxaporpyrin remain equivalent as a single resonance has been detected for each *meso*-phenyl ring. The plots of the temperature dependence of chemical shifts demonstrate pronounced deviation from the Curie behavior (Figure 8).

While the spectroscopic properties of the newly detected intermediate are consistent with the (OTPP)Fe^{I} stoichiometry, the oxidation states of the iron and the 21-oxaporphyrin ligand remain to be analyzed. Two alternative electronic structures can be considered in analogy to two-electron reduction products of iron(III) regular porphyrins.[33,34,51−55]

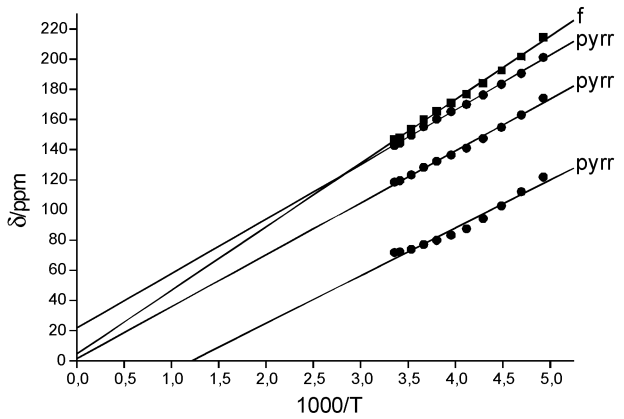

Figure 8. Curie plot (chemical shifts versus 1/*T*) for pyrrole and furan resonances of (OTPP)Fe^{I} (toluene-d_8). The solid lines are for illustrative purposes only.

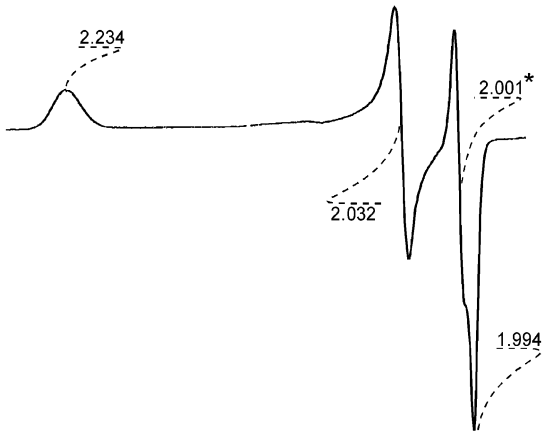

Figure 9. EPR spectrum (X-band, toluene-d_8, 77 K). The signal of the residual radical is marked with an asterisk. Conditions: microwave frequency ν = 9.5750 GHz, microwave power 20 mW, modulation amplitude 4.88 G, modulation frequency 100 kHz.

They are differentiated by localization of an added electron leading either to iron(I) 21-oxaporphyrin or iron(II) 21-oxaporphyrin π anion radical complexes, that is, (OTPP)Fe^{I} or (OTPP$^{\bullet-}$)Fe^{II}, respectively. The EPR spectroscopy brings a valuable insight into the electronic structure of (OTPP)Fe^{I} at 77 K. The relevant EPR spectrum of (OTPP)Fe^{I} as frozen toluene-d_8 solution is shown in Figure 9. The species has been prepared in the 5 mm NMR tube by addition of the PhMgBr to (OTPP)Fe^{III}Cl$_2$ at 205 K. The composition of the solution has been confirmed by ^{1}H NMR spectroscopy before and after the EPR measurements. The species reveals the remarkable anisotropy of the **g** tensor $g_1 = 2.234$, $g_2 = 2.032$, $g_3 = 1.990$. This indicates a $(d_{xy})^2(d_{xz})^2(d_{yz})^2(d_{z^2})^1(d_{x^2-y^2})^0$ electronic state for the reduction product as detected at 77 K. The analogous EPR parameters have been reported for other low-spin d^7 complexes including iron(I) porphyrins.[39,56]

Electronic Structure of (OTPP)Fe: ^{1}H NMR Studies. ^{1}H NMR spectra of the two-electron reduced iron(III) porphyrins are diagnostic for determination of a ground electronic state. Depending on iron porphyrin substitution,

(50) Li, Z.; Goff, H. M. *Inorg. Chem.* **1992**, *31*, 1547.
(51) Reed, C. A. *Adv. Chem. Ser.* **1981**, *201*, 333.
(52) Mashiko, T.; Reed, C. A.; Haller, K. J.; Scheidt, W. R. *Inorg. Chem.* **1984**, *23*, 3192.
(53) Sano, S.; Suguira, Y.; Maeda, Y.; Ogawa, S. Morishima, I. *J. Am. Chem. Soc.* **1981**, *103*, 2888.
(54) Hickman, D. L.; Shirazi, G.; Goff, H. M. *Inorg. Chem.* **1985**, *24*, 563.
(55) Yamaguchi, K.; Morishima, I. *Inorg. Chem.* **1992**, *31*, 3216.
(56) Kadish, K. M.; Van Caemelbecke, E.; D'Souza, F.; Lin, M.; Nurco, D. J.; Medforth, C. J.; Forsyth, T. P.; Krattinger, B.; Smith, K. M.; Fukuzumi, S.; Nakanishi, I.; Shelnut, J. A. *Inorg. Chem.* **1999**, *38*, 2188.

the following possibilities have been realized (the significant paramagnetic shifts are given for ca. 293 K in parentheses): (a) low-spin iron(I) $(d_{xy})^2(d_{xz})^2(d_{yz})^2(d_{z^2})^1(d_{x^2-y^2})^0$ ([(TPP)Fe^I] β-H 29 ppm),[54] (b) resonance structures between two low-spin canonic forms $(P^{\bullet-})Fe^{II} \leftrightarrow PFe^I$ (e.g., iron porphyrin containing electron-withdrawing substituents, $[(CN)_4TPP)Fe]^-$ pyrrole 11 ppm, *o*-H −0.8, *m*-H 13.7; *p*-H 3.4 ppm),[55] (c) high-spin ferrous iron(II) $(d_{xy})^2(d_{xz})^2(d_{yz})^1(d_{z^2})^1(d_{x^2-y^2})^1$ coupled to a π anion radical $[d_3$-(5-NO_2OEP)Fe]$^-$ α-CH_2 60−40, *meso* −58(2), −210(1)).[55]

Thus, (OTPP)Fe^I demonstrates spectroscopic features never seen for iron tetraarylporphyrins obtained as a product of two-electron reduction of iron(III) tetraarylporphyrins. Importantly, the ^{1}H NMR spectroscopic pattern measured in the 203−273 K temperature range remains in a striking contradiction to the EPR data (the frozen toluene-d_8 glass, 77 K), which are unambiguously consistent with the $(d_{xy})^2(d_{xz})^2(d_{yz})^2(d_{z^2})^1(d_{x^2-y^2})^0$ ground electronic state. Definitely, raising the temperature resulted in the fundamental change of the electronic structure.

As expected, the number of resonances for (OTPP)Fe^I reflects the lower symmetry of 21-oxaporphyrin. Of particular significance are the remarkable downfield shifts of the pyrrole and furan resonances detected for (OTPP)Fe^I. The pattern appears to result from a domination of the σ delocalization pathways moderated by some contribution of the π mechanism. Unequivocally, the unpaired electron is located on the $d_{x^2-y^2}$ orbital. In general, three electronic structures or their combination are consistent with the detected paramagnetic shifts: (a) high-spin iron(II) radical $(d_{xy})^2(d_{xz})^1(d_{yz})^1(d_{z^2})^1(d_{x^2-y^2})^1$ coupled to 21-oxaporphyrin radical ($S = {}^3/_2$ or $S = {}^5/_2$), (b) high-spin iron(I) $(d_{xy})^2(d_{xz})^2(d_{yz})^1(d_{z^2})^1(d_{x^2-y^2})^1$ ($S = {}^3/_2$), (c) low-spin iron(I) $(d_{xy})^2(d_{xz})^2(d_{yz})^2(d_{z^2})^0(d_{x^2-y^2})^1$ ($S = {}^1/_2$).

Actually, the first case has a precedent exemplified by d_3-[(5-NO_2OEP)Fe]$^-$.[56] However, because of differences in substitution, the direct spectroscopic comparison between tetraaryl- and octaethylporphyrin derivatives is not possible. One can expect that the large π spin density at the *meso* position seen for $[d_3$-(5-NO_2OEP)Fe]$^-$ will be translated into the relatively large isotropic shifts of *meso*-aryl protons with sign alteration between *meta* and *para* (*ortho*) resonances.[33] Accordingly, the large downfield shift of the α-methylene protons can be translated into the large downfield shift from replacing the β-H protons, presuming that the σ contribution dominates the contact shift. The π delocalization effect is less predictable. At this stage of discussion, we may conclude that the contact shift of β-H results from the simultaneous delocalization in σ as well as both filled and vacant molecular orbitals related to the 3e(π) and 4e(π*) orbitals of the regular porphyrin. Ultimately, the upfield π contribution due to delocalization in the π orbitals may be overshadowed by the strong downfield contribution of the σ mechanism.[38]

The high-spin d^7 iron(I) allows both σ and π delocalization routes as well. Such an electronic structure was never characterized for iron(I) porphyrins. As an appropriate ^{1}H NMR reference, one can suggest high-spin d^7 cobalt(II) complexes, (NCH_3TPP)Co^{II}Cl and (STPP)Co^{II}Cl, where the marked downfield shift of the pyrrole resonances was observed.[57,58]

Conclusions. This study broadens our understanding of the coordination of iron in a porphyrin and porphyrin-like environment. The essential similarities of iron porphyrin and iron 21-oxaporphyrin complexes have been established. Both form high-spin five-coordinate complexes, μ-oxo bridged diiron(III) complexes, and low spin six-coordinate iron(III) complexes with strong field ligands. In addition, σ-alkyliron(II) complexes have been detected in each case. Finally, two-electron reduction of iron(III) porphyrin and iron(III) 21-oxaporphyrin gave corresponding iron(I) compounds. There is a considerable analogy in the magnetic and ^{1}H NMR properties despite inherent lower symmetry of the 21-oxaporphyrin within each iron(*n*) 21-oxaporphyrin−iron(*n*) regular porphyrin pair. Actually, the best parallel can be drawn between iron 21-oxaporphyrin and iron *N*-methylporphyrin despite the difference in coordination mode of the modified five-membered rings (*N*-methylated pyrrole, side-on; furan, in-plane). Importantly, once the symmetry has been lowered accompanied by a change of the macrocyclic charge from −2 to −1, the stabilization of lower oxidation states occurred. This is demonstrated for iron *N*-methylporphyrin and iron 21-oxaporphyrin in comparison to iron porphyrins as clearly seen at the iron(III)/iron(II) reduction level.

Experimental Section

Materials. 5,10,15,20-Tetraphenyl-21-oxaporphyrin (OTPP)H and its derivative deuterated at β-pyrrole positions (OTPP-d_6)H were synthesized as described previously.[6] C_6H_5MgBr, *n*-buthyllithium, and sodium borohydride were purchased from Aldrich.

(OTPP)$Fe^{III}Cl_2$. A solution of 200 mg (1 mmol) of iron(II) chloride tetrahydrate in 5 mL of methanol was added to a solution of 50 mg (0.07 mmol) of 5,10,15,20-tetraphenyl-21-oxaporphyrin in 40 mL of chloroform. After 20 min, the solvent was removed under reduced pressure. The solid residue was extracted with dichloromethane, and the dichloromethane solution was separated from the remaining solid by filtration. Recrystallization from dichloromethane/hexane (50/50) produced 37 mg of (OTPP)Fe^{III}-Cl_2 (yield 63%). UV−vis λ [nm] (log ϵ) = 412 (4.70), 435 (4.59), 568 (3.80), 597 (3.64). MS (ESI, *m*/*z*) 705.1241 (705.1348 calcd for $(C_{44}H_{28}N_3OFeCl)^+$, the most intensive peak). (OTPP-d_6)Fe^{III}-Cl_2 was obtained the same way using (OTPP-d_6)H.

(OTPP)Fe^{II}Cl. (OTPP)$Fe^{III}Cl_2$ (20 mg) was dissolved in chloroform and energetically stirred with zinc amalgam (2 h). The reducing reagent was filtered off, and the solution of (OTPP)Fe^{II}-Cl was taken to dryness under reduced pressure. Conversion into the iron(II) compound proceeded quantitatively. Yield 19 mg. UV−vis λ [nm] (log ϵ) = 426 (4.83), 442 (4.82), 546(3.83), 588 (3.73), 633 (3.39). MS (ESI, *m*/*z*) 670.1576 (670.1696 calcd for $(C_{44}H_{28}$-$N_3OFe)^+$, the most intensive peak).

X-ray Data Collection and Refinement. Crystals of (OTPP)-$Fe^{III}Cl_2$ were prepared by diffusion of hexane into the chloroform solution contained in a thin tube.

Crystal data for (OTPP)$Fe^{III}Cl_2$ are given in Table 2, together with refinement details. The crystal was mounted on glass fiber and then flash-frozen to 100 K (Oxford Cryosystem-Cryostream

(57) Latos-Grażyński, L. *Inorg. Chem.* **1985**, *24*, 1105.
(58) Lisowski, J.; Latos-Grażyński, L. Unpublished results, see ref 2, p 404.

Table 2. Crystal Data for (OTPP)$Fe^{III}Cl_2$ with Refinement Details

	(OTPP)$Fe^{III}Cl_2$
formula	$C_{44}H_{28}N_3OFeCl_2$
fw	741.44
a,Å	13.524(2)
b,Å	13.524(2)
c,Å	9.763(2)
V, Å^3	1785.6(5)
Z,	2
D_{calcd}, g·cm^{-3}	1.379
cryst syst	tetragonal
space group	*I*4/*m*
μ, mm^{-1}	0.612
abs correction	not applied
T_{min}	0.8621
T_{max}	0.9584
T, K	100(2)
θ range	$3.96 \le \theta \le 28.55$
hkl range	$-17 \le h \le 17$
	$-17 \le k \le 17$
	$-13 \le l \le 3$
reflns measured	1133
reflns unique, $I > 2\sigma(I)$	1056
params/restraints	72/0
S	1.074
R1[a]	0.0801
wR2[a]	0.1912

[a] $R1 = \sum||F_o| - |F_c||/\sum|F_o|$, $wR2 = [\sum[w(F_o^2 - F_c^2)^2/\sum[w(F_o^2)^2]]^{1/2}$.

Cooler). Preliminary examination and intensity data collections were carried out on a Kuma KM4CCD κ-axis diffractometer with graphite-monochromated Mo Kα radiation. The data were corrected for Lorentz and polarization effects. No absorption correction was applied. Data reduction and analysis were carried out with the Kuma Diffraction (Wrocław) programs. The structures were solved by heavy atom methods (program SHELXS97)[59] and refined by the full-matrix least-squares method on all F^2 data using the SHELXL97 programs.[60] The disorder exists in the complex (OTPP)$Fe^{III}Cl_2$. Molecules have four different orientations (1:1:1:1) in the unit cell, but the Fe(1), Cl(1), and Cl(2) atoms have identical coordinates in each case. These molecules differ by rotation along the Fe(1)−Cl-(1) bond by 90°. Non-hydrogen atoms from the molecule with primary orientation were refined with anisotropic displacement parameters and isotropically in the molecule with secondary orientation using instruction SAME; coordinates of the hydrogen atoms were calculated using the geometry of molecules and were refined as riding groups for all orientations of (OTPP)$Fe^{III}Cl_2$. The carbon-bonded hydrogen atoms were included in the calculated positions and refined using a riding model.

Instrumentation. NMR spectra were recorded on a 500 MHz Bruker Avance spectrometer equipped with a broadband inverse gradient probehead. Proton data are referenced to the residual solvent signal. EPR spectra were obtained with a Bruker ESP 300E spectrometer. The magnetic field was calibrated with a proton magnetometer and EPR standards.

Electrochemical measurements were performed in CH_2Cl_2 with tetrabutylammonium perchlorate as supporting electrolyte. Cyclic voltammograms were recorded for the potential scan rate ranging from 0.02 to 0.5 V/s using the EA9C (MIM, Kraków, Poland) apparatus. The Pt-disk working electrode, Pt-wire auxiliary electrode, and the Ag/AgCl reference electrode were utilized.

Sample Preparation. A sample of 3 mg of (OTPP)$Fe^{III}Cl_2$ was dissolved in 0.5 cm^3 of oxygen-free toluene-d_8 directly in an NMR tube capped with a rubber septum cap. The sample was cooled to 193 K in the acetone slush bath, and the respective reagent (the Grignard reagent, butyllithium) was titrated into the NMR tube using a microsyringe. The sample was shaken vigorously and then immediately transferred to the ^{1}H NMR spectrometer which was maintained at 205 K. Samples of the (OTPP)Fe^{I} complex for the EPR measurements were prepared by addition of PhMgBr to the solution of (OTPP)$Fe^{III}Cl_2$ directly in the ^{1}H NMR tube which was used in both experiments.

Acknowledgment. Financial support of the Polish State Committee for Scientific Research KBN (Grant 4T 09A 14722) and the Foundation for Polish Science is kindly acknowledged.

Supporting Information Available: Crystallographic data in CIF format. VT NMR data for (OTPP)$Fe^{III}Cl_2$, (OTPP)$Fe^{II}Cl$, and (OTPP)$Fe^{III}(CN)_2$ and NMR characteristics of $[(OTPP)Fe^{III}(CN)_2]^-$. This material is available free of charge via the Internet at http://pubs.acs.org/.

IC025718P

(59) Sheldrick, G. M. *SHELXS97, program for solution of crystal structures*; University of Göttingen: Göttingen, Germany, 1997.
(60) Sheldrick, G. M. *SHELXL97, program for crystal structure refinement*; University of Göttingen: Göttingen, Germany, 1997.